

# Permanent deflection identification of non-linear structures undergoing seismic excitation using adaptive LMS filters

M. Nayyerloo, J. G. Chase & X. Q. Chen

*Department of Mechanical Engineering, University of Canterbury, Christchurch.*

G. A. MacRae & M. Moghaddasi

*Department of Civil and Natural Resources Engineering, University of Canterbury, Christchurch.*



2009 NZSEE  
Conference

**ABSTRACT:** Structural Health Monitoring (SHM) algorithms based on Adaptive Least Mean Square (LMS) filtering theory can directly identify time-varying changes in structural stiffness in real time, are robust to noise, and computationally efficient. Common modal or wavelet methods are less robust to noise and small levels of damage. However, the best metrics of seismic structural damage are related to permanent and plastic deformations, which no reported methods identify. This research uses LMS-based SHM methods with a baseline non-linear Bouc-Wen structural model to directly identify permanent deflection and changes in stiffness (modelling or construction error), in real-time. The algorithm is validated, *in silico*, on an equivalent single degree of freedom of a non-linear 5-storey shear-type concrete structure using MATLAB<sup>®</sup>. The Cape Mendocino ground motion is scaled to a level that causes permanent deflection to show the algorithm's capability. For the simulated structure, the algorithm identifies stiffness changes to within 10% of true value in 2.0 seconds, and permanent deflection is identified to within 0.5% of the actual as-modelled value.

## 1 INTRODUCTION

Structural health monitoring (SHM) is the process of comparing the current state of a structure's condition relative to a baseline state to detect the existence, location, and degree of likely damage after a damaging input. Many current vibration-based SHM methods are based on the idea that changes in modal parameters; frequencies, mode shapes and modal damping, are a result of damage or decay. These methods are typically more applicable to steel-frame and bridge structures where vibration response is highly linear (Chase et al., 2004). However, a major drawback of many approaches is their inability to be implemented in real-time, on a sample-to-sample basis as the event occurs. Further, their reliance on modal properties has potential problems. In some cases, modal properties are not robust in the presence of strong noise and insensitive to small amounts of damage (Hou et al., 2000). Adaptive fading Kalman filters (Loh & Lin, 2000) and adaptive  $H_\infty$  filter techniques (Sato & Qi, 1998) which achieve real-time or near real-time results, provide identification of modal parameters in real time, but come with significant computational cost and complexity. Moreover, like other linear approaches they are not applicable to the typical non-linearities found in seismic structural responses.

In contrast, direct identification of changes in stiffness and/or permanent deflection would offer the post-earthquake outputs desired by engineers. Least Mean Squares (LMS) based SHM has been used for a benchmark problem (Chase et al., 2004), and also for a non-linear rocking structure (Chase et al., 2005), to directly identify changes in structural stiffness only. They are robust with fast convergence and low computational cost. However, they require full state measurement and do not identify plastic and permanent deflections. The goal is to obtain these plastic and permanent deflections in real time in a computationally efficient and robust fashion. Model-based methods combined with modern filtering

theory offer that opportunity.

## 2 PROBLEM DEFINITION

A seismically excited non-linear structure can be modelled as:

$$\mathbf{M} \cdot \{\ddot{\mathbf{v}}\} + \mathbf{C} \cdot \{\dot{\mathbf{v}}\} + \mathbf{K}_T(t) \cdot \{\mathbf{v}\} = -\underline{\mathbf{M}} \cdot \ddot{\mathbf{x}}_g \quad (1)$$

where  $\mathbf{M}$ ,  $\mathbf{C}$ , and  $\mathbf{K}_T$  are the mass, damping, and tangent stiffness matrices of the model respectively,  $\{\mathbf{v}\}$ ,  $\{\dot{\mathbf{v}}\}$ , and  $\{\ddot{\mathbf{v}}\}$  are the displacement, velocity, and acceleration vectors, respectively, and  $\ddot{\mathbf{x}}_g$  is the ground motion acceleration. The tangent stiffness matrix of a hysteretic structure can be represented using Bouc-Wen model. The dimensionless hysteretic component of the  $i^{th}$  storey,  $z_i$ , is governed by the following first order non-linear differential equation (Constantinou & Tadjbakhsh, 1985):

$$\dot{z}_i(t) = \frac{A_i \dot{r}_i(t) - \beta_i |\dot{r}_i(t)| |z_i|^{n_i-1} z_i - \gamma_i \dot{r}_i(t) |z_i|^{n_i}}{Y_i}, i = 1, \dots, N \quad (2)$$

where  $A_i$  (usually 1.0),  $\beta_i$  (0.1 to 0.9),  $\gamma_i$  (-0.9 to 0.9), and  $n_i$  (1 to 3, usually 1) are stiffness, loop fatness, loop pinching, and abruptness parameters in a classical Bouc-Wen model, respectively. Further,  $n_i$ , the power factor, determines the curve from elastic to plastic force-deflection behaviour of each storey.  $\dot{r}_i(t)$  is the velocity of storey  $i$  relative to storey  $i-1$ ,  $Y_i$  is the yield displacement of  $i^{th}$  story, and  $N$  is the number of stories. The five dimensionless parameters,  $A_i$ ,  $\beta_i$ ,  $\gamma_i$ ,  $n_i$ , and  $\alpha_i$  determine the hysteresis loops shape. Neither degradation nor pinching of hysteresis is accounted for by the classical Bouc-Wen model. Over the years, this classical model has been modified to accommodate changes in hysteresis loops arising from deteriorating systems, and the contemporary model can be found in (Baber & Noori, 1986). In this study, the classical Bouc-Wen model has been used, and only non-linearities arising from the hysteresis behaviour of the building has been considered.

Using Equation (2), the tangent stiffness matrix of a 4-DOF four-storey shear-type structure, as an example for the tangent stiffness matrix of a hysteretic structure in MDOF case, can be written as:

$$\mathbf{K}_T = \begin{bmatrix} [\alpha_1 + (1-\alpha_1)Y_1 \frac{\Delta \sigma_1}{\Delta \tau_1}(k_0)_1 + \alpha_2(k_0)_2] & -[\alpha_2 + (1-\alpha_2)Y_2 \frac{\Delta \sigma_2}{\Delta \tau_2}(k_0)_2] & 0 & 0 \\ -\alpha_2(k_0)_2 & [\alpha_2 + (1-\alpha_2)Y_2 \frac{\Delta \sigma_2}{\Delta \tau_2}(k_0)_2 + \alpha_3(k_0)_3] & -[\alpha_3 + (1-\alpha_3)Y_3 \frac{\Delta \sigma_3}{\Delta \tau_3}(k_0)_3] & 0 \\ 0 & -\alpha_3(k_0)_3 & [\alpha_3 + (1-\alpha_3)Y_3 \frac{\Delta \sigma_3}{\Delta \tau_3}(k_0)_3 + \alpha_4(k_0)_4] & -[\alpha_4 + (1-\alpha_4)Y_4 \frac{\Delta \sigma_4}{\Delta \tau_4}(k_0)_4] \\ 0 & 0 & -\alpha_4(k_0)_4 & [\alpha_4 + (1-\alpha_4)Y_4 \frac{\Delta \sigma_4}{\Delta \tau_4}(k_0)_4] \end{bmatrix} \quad (3)$$

If damage occurs in the structure from an earthquake, or any other source of damaging excitation, structural properties, such as natural frequency and stiffness may also change, and may be time-varying. For the damaged structure, the equations of motion can be re-defined as:

$$\mathbf{M} \cdot \{\ddot{\mathbf{v}}\} + \mathbf{C} \cdot \{\dot{\mathbf{v}}\} + (\overline{\mathbf{K}}_T + \Delta \overline{\mathbf{K}}_T) \cdot \{\mathbf{v}\} = -\underline{\mathbf{M}} \cdot \ddot{\mathbf{x}}_g \quad (4)$$

where  $\{\ddot{\mathbf{v}}\}$ ,  $\{\dot{\mathbf{v}}\}$ , and  $\{\mathbf{v}\}$  are the measured responses of the damaged structure,  $\overline{\mathbf{K}}_T$ , is the tangent stiffness matrix of the damaged structure from Equation (3) using damaged structural responses, and  $\Delta \overline{\mathbf{K}}_T$  contains changes in the tangent stiffness of the structure due to modelling or construction error damage and can be a function of time. Using Equation (3),  $\Delta \overline{\mathbf{K}}_T$  due to modelling or construction damage can be written as:

$$\Delta\bar{\mathbf{K}}_T = \begin{bmatrix} [\alpha_1 + (1-\alpha_1)Y_1 \frac{\Delta\bar{z}_1}{\Delta\bar{r}_1}](\Delta k_0)_1 + \alpha_2(\Delta k_0)_2 & -[\alpha_2 + (1-\alpha_2)Y_2 \frac{\Delta\bar{z}_2}{\Delta\bar{r}_2}](\Delta k_0)_2 & 0 & 0 \\ -\alpha_2(\Delta k_0)_2 & [\alpha_2 + (1-\alpha_2)Y_2 \frac{\Delta\bar{z}_2}{\Delta\bar{r}_2}](\Delta k_0)_2 + \alpha_3(\Delta k_0)_3 & -[\alpha_3 + (1-\alpha_3)Y_3 \frac{\Delta\bar{z}_3}{\Delta\bar{r}_3}](\Delta k_0)_3 & 0 \\ 0 & -\alpha_3(\Delta k_0)_3 & [\alpha_3 + (1-\alpha_3)Y_3 \frac{\Delta\bar{z}_3}{\Delta\bar{r}_3}](\Delta k_0)_3 + \alpha_4(\Delta k_0)_4 & -[\alpha_4 + (1-\alpha_4)Y_4 \frac{\Delta\bar{z}_4}{\Delta\bar{r}_4}](\Delta k_0)_4 \\ 0 & 0 & -\alpha_4(\Delta k_0)_4 & [\alpha_4 + (1-\alpha_4)Y_4 \frac{\Delta\bar{z}_4}{\Delta\bar{r}_4}](\Delta k_0)_4 \end{bmatrix} \quad (5)$$

Identifying the  $\Delta\bar{\mathbf{K}}_T$  term enables the structure's condition to be directly monitored without using modal parameters.

To determine  $\Delta\bar{\mathbf{K}}_T$  using adaptive LMS, following the method proposed in (Chase et al., 2004), a new form of  $\Delta\bar{\mathbf{K}}_T$  is defined with time-varying scalar parameters,  $\hat{\alpha}_i$ , to be identified using the LMS filter. For instance,  $\Delta\bar{\mathbf{K}}_T$  for a 4-DOF four-story shear building is sub-divided into four matrices to allow independent identification of changes in stiffness of each story i.e.  $(\Delta k_0)_1$ ,  $(\Delta k_0)_2$ ,  $(\Delta k_0)_3$ , and  $(\Delta k_0)_4$ :

$$\Delta\bar{\mathbf{K}}_T = \hat{\alpha}_1 \begin{bmatrix} \alpha_1 + (1-\alpha_1)Y_1 \frac{\Delta\bar{z}_1}{\Delta\bar{r}_1} & 0 & 0 & 0 \\ 0 & 0 & 0 & 0 \\ 0 & 0 & 0 & 0 \\ 0 & 0 & 0 & 0 \end{bmatrix} + \hat{\alpha}_2 \begin{bmatrix} \alpha_2 & -[\alpha_2 + (1-\alpha_2)Y_2 \frac{\Delta\bar{z}_2}{\Delta\bar{r}_2}] & 0 & 0 \\ -\alpha_2 & \alpha_2 + (1-\alpha_2)Y_2 \frac{\Delta\bar{z}_2}{\Delta\bar{r}_2} & 0 & 0 \\ 0 & 0 & 0 & 0 \\ 0 & 0 & 0 & 0 \end{bmatrix} + \hat{\alpha}_3 \begin{bmatrix} 0 & 0 & 0 & 0 \\ 0 & \alpha_3 & -[\alpha_3 + (1-\alpha_3)Y_3 \frac{\Delta\bar{z}_3}{\Delta\bar{r}_3}] & 0 \\ 0 & -\alpha_3 & \alpha_3 + (1-\alpha_3)Y_3 \frac{\Delta\bar{z}_3}{\Delta\bar{r}_3} & 0 \\ 0 & 0 & 0 & 0 \end{bmatrix} + \hat{\alpha}_4 \begin{bmatrix} 0 & 0 & 0 & 0 \\ 0 & 0 & 0 & 0 \\ 0 & 0 & \alpha_4 & -[\alpha_4 + (1-\alpha_4)Y_4 \frac{\Delta\bar{z}_4}{\Delta\bar{r}_4}] \\ 0 & 0 & -\alpha_4 & \alpha_4 + (1-\alpha_4)Y_4 \frac{\Delta\bar{z}_4}{\Delta\bar{r}_4} \end{bmatrix} \quad (6)$$

where

$$\hat{\alpha}_1 = (\Delta k_0)_1, \hat{\alpha}_2 = (\Delta k_0)_2, \hat{\alpha}_3 = (\Delta k_0)_3, \hat{\alpha}_4 = (\Delta k_0)_4 \quad (7)$$

hence equations (6) can be expressed as:

$$\Delta\bar{\mathbf{K}}_T = \sum_{i=1}^n \hat{\alpha}_i \mathbf{K}_i \quad (8)$$

where  $n$  is the number of degrees of freedom (DOF) of the model, and  $\mathbf{K}_i$  is the corresponding time-varying matrix to  $i^{\text{th}}$  DOF in Equation (6). Rewriting (4) using (6)-(8) yields:

$$\sum_{i=1}^n \hat{\alpha}_i \mathbf{K}_i \cdot \{\bar{\mathbf{v}}\} = -\underline{\mathbf{M}} \cdot \ddot{\mathbf{x}}_g - \underline{\mathbf{M}} \cdot \{\ddot{\bar{\mathbf{v}}}\} - \underline{\mathbf{C}} \cdot \{\dot{\bar{\mathbf{v}}}\} - \bar{\mathbf{K}}_T \cdot \{\bar{\mathbf{v}}\} \quad (9)$$

In Equation (9), responses of the damaged structure  $\{\ddot{\bar{\mathbf{v}}}\}$ ,  $\{\dot{\bar{\mathbf{v}}}\}$ , and  $\{\bar{\mathbf{v}}\}$  are measured. The matrix  $\bar{\mathbf{K}}_T$  at each time step is calculated using Equations (2) and (3). The  $Y_i \frac{\Delta\bar{z}_i}{\Delta\bar{r}_i}$  term in  $\bar{\mathbf{K}}_T$  and  $\mathbf{K}_i$  matrices can be re-defined by introducing a hysteretic displacement,  $h_i$ , for each storey as:

$$h_i = Y_i z_i, i = 1, \dots, N \quad (10)$$

where  $Y_i$  and  $z_i$  are the yield displacement and the hysteretic component of the  $i^{\text{th}}$  storey, respectively. Assuming  $A_i=1$ ,  $\beta_i=0.5$ , and  $\gamma_i=0.5$  in Equation (2),  $\frac{dh_i}{dr_i}$  can be written as:

$$\frac{dh_i}{dr_i} = 1 - 0.5 \left[ 1 + \text{sign}(\dot{r}_i(t)h_i(t)) \right] \left| \frac{h_i(t)}{Y_i} \right|^{n_i}, i = 1, \dots, N \quad (11)$$

as,

$$\dot{h}_i = \frac{dh_i}{dr_i} \cdot \dot{r}_i, i = 1, \dots, N \quad (12)$$

therefore,  $Y_i \frac{\Delta \bar{z}_i}{\Delta \bar{r}_i}$  term for the damaged system can be obtained from Equation (13):

$$Y_i \frac{\Delta \bar{z}_i}{\Delta \bar{r}_i} = 1 - 0.5 \left[ 1 + \text{sign}(\dot{\bar{r}}_i(t)\bar{h}_i(t)) \right] \left| \frac{\bar{h}_i(t)}{Y_i} \right|^{n_i}, i = 1, \dots, N \quad (13)$$

where  $\bar{h}_i$  and  $\bar{r}_i$  are the damaged hysteretic displacement of storey  $i$  and the damaged relative displacement between storey  $i$  and storey  $i-1$ , respectively.  $\bar{h}_i$  can be calculated from Equation (14) using Equation (12) for the damaged structure and assuming constant  $\dot{\bar{h}}_i$  at each time step.

$$\bar{h}_i(t + \Delta t) = \dot{\bar{r}}_i(t) \left\{ 1 - 0.5 \left[ 1 + \text{sign}(\dot{\bar{r}}_i(t)\bar{h}_i(t)) \right] \left| \frac{\bar{h}_i(t)}{Y_i} \right|^{n_i} \right\} \Delta t + \bar{h}_i(t), i = 1, \dots, N \quad (14)$$

where  $\Delta t$  is the time step.

In this fashion, plastic displacement in the Bouc-Wen model is defined as:

$$D_i(t) = \bar{r}_i(t) - \bar{h}_i(t), i = 1, \dots, N \quad (15)$$

where  $D_i(t)$  is the plastic deformation of storey  $i$ .

The damaged structure stiffness, or the effective stiffness changes due to non-linear behaviour such as hysteresis, can then be determined by identifying the  $\hat{\alpha}_i$  at every discrete time step using Equation (16).

$$\sum_{i=1}^n \hat{\alpha}_i \mathbf{K}_i \cdot \bar{\mathbf{v}}_k = -\mathbf{M} \cdot (\ddot{\mathbf{x}}_g)_k - \mathbf{M} \cdot \ddot{\bar{\mathbf{v}}}_k - \mathbf{C} \cdot \dot{\bar{\mathbf{v}}}_k - \bar{\mathbf{K}}_T \cdot \bar{\mathbf{v}}_k = y_k \quad (16)$$

where  $(\ddot{\mathbf{x}}_g)_k$  is the input ground acceleration at time  $k$ , and  $\ddot{\bar{\mathbf{v}}}_k$ ,  $\dot{\bar{\mathbf{v}}}_k$  and  $\bar{\mathbf{v}}_k$  are the measured acceleration, velocity, and displacement of the damaged structure at time  $k$ , respectively. Matrices of  $\bar{\mathbf{K}}_T$  and  $\mathbf{K}_i$  are calculated sample-to-sample using Equations (3) and (6) with the measured damaged structural responses. The elements of the vector signal  $y_k$  can be readily modelled in real-time using an adaptive LMS filter so that the coefficients  $\hat{\alpha}_i$ , changes in linear elastic stiffness of each storey due to modelling or construction damage, can be readily determined.

### 3 ADAPTIVE LMS FILTERING

Adaptive filters are digital filters with coefficients that can change over time. The general idea is to update filter coefficients and assess how well the existing coefficients are performing in modelling a noisy signal, and then adapt the coefficient values to improve performance. The least mean squares (LMS) algorithm is one of the most widely used of all the adaptive filtering algorithms and is relatively simple to implement. It is an approximation of the Steepest Descent Method using an estimator of the gradient instead of its actual value, considerably simplifying the calculations and to be

readily performed in real-time applications. The goal in this case is to model the individual, scalar elements of the signal  $y_k$  of (16) using the adaptive LMS filter.

In adaptive LMS filtering, the coefficients are adjusted from sample-to-sample to minimize the mean square error (MSE), between a measured noisy scalar signal and its modelled value from the filter.

$$\hat{e}_k = \hat{y}_k - W_k^T X_k = \hat{y}_k - \sum_{i=0}^{m-1} w_k(i) x_{k-i} \quad (17)$$

where  $W_k$  is the adjustable filter coefficient vector or weight vector at time  $k$ ,  $\hat{y}_k$  is the measured noisy scalar signal at time  $k$ , to be modelled or approximated,  $X_k$  is the input vector to the filter, model of current and previous filter inputs,  $x_{k-i}$ , so  $W_k^T X_k$  is the vector dot product output from the filter at time  $k$  to model a scalar signal  $\hat{y}_k$ , and  $m$  is the number of prior time steps or taps considered. The Widrow–Hopf LMS algorithm for updating the weights to minimize the error,  $e_k$ , is defined as (Ifeachor & Jervis, 1993):

$$W_{k+1} = W_k + 2\mu \cdot e_k \cdot X_k \quad (18)$$

where  $\mu$  is a positive scalar, called step size, that controls the stability and rate of convergence.

To identify  $\Delta \bar{\mathbf{K}}_T$  at time  $k$ , using LMS adaptive filters we will follow the One-Step method (Chase et al., 2004) and re-write Equation (17) in matrix form by substituting  $W_k^T X_k$  with its equivalent from Equation (16):

$$e_k = y_k - \sum_{j=0}^{m-1} \sum_{i=1}^n \hat{\alpha}_{ij} \mathbf{K}_i \cdot \bar{v}_{k-j} \quad (19)$$

Minimizing the mean square error (MSE) with respect to  $\hat{\alpha}_{ij}$  using Equation (18) yields the following weight update formula for the SHM problem:

$$w_{k+1} = w_k + 2\mu e_k^T \mathbf{K}_i \cdot \bar{v}_{k-j} \quad (20)$$

Summing  $\hat{\alpha}_{ij}$  over  $j$ , yields the  $\hat{\alpha}_i$ , changes in stiffness of each story in Equation (16).

#### 4 INPUTS TO THE SHM PROBLEM

Inputs to this SHM problem are acceleration, velocity, and displacement of the structure. Acceleration can be easily measured with low cost accelerometers at high sampling rates. Due to practical constraints, direct high speed measurement of displacement and velocity is not typically possible. A high speed displacement sensor would provide displacement, and could be used to derive velocity at low added computational cost. Estimating the velocity using both acceleration and displacement data would provide a more precise estimation of the velocity. To measure displacement of a real structure at high rates up to tens of kHz, line scan cameras can be used, although this paper proposes but does not explore the method proposed in (Lim M. & Lim J., 2008).

#### 5 SIMULATED CASE STUDY STRUCTURE

The simulated structure is an equivalent single degree of freedom (ESDOF) of one of the moment-resisting frames in long-direction of a five-story concrete building. The plan view of a typical floor of the building is shown in Figure 1. The floor system consists of 200 series precast hollow-core floor units having a 65 mm topping spanning on long direction of each floor. The seismic weight per floor is 1692 kN for roof level and 2067 kN for other levels. Each storey has 3.8 m height, and the frame system is designed according to the New Zealand Concrete Structures Standard (NZS 3101) using the displacement-based design approach to sustain a target drift level of 2% under a 500-year return period earthquake.

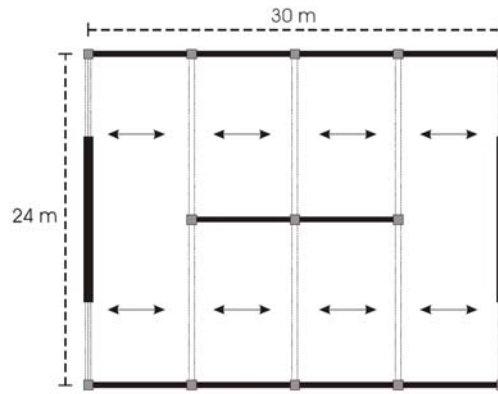


Figure 1. Plan view of the simulated 5-storey shear-type concrete building

Figure 2 shows the push-over analysis results of the building. Ruaumoko was used to perform the analysis to determine the total linear stiffness (27300 kN), the bi-linear factor (0.065), and the yield displacement (46.5 mm) of the building.

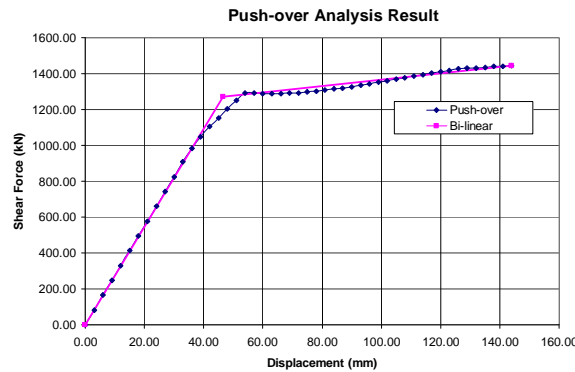


Figure 2. Push-over analysis results of the simulated building using Ruaumoko

Non-linear dynamic analysis using a Bouc-Wen hysteretic model was performed in MATLAB<sup>®</sup> to represent the non-linear hysteretic behaviour of the structure, and the simulated structural responses from MATLAB<sup>®</sup> was used to provide proof of concept and quantify the accuracy of the identified parameters, changes in linear elastic stiffness of each storey, and identified plastic and permanent displacements. In simulating the structural responses, 5% constant damping was considered, and the building was given a shaping parameter of  $n=2$  to provide realistic non-linear structural behaviour.

The developed SHM algorithm was implemented in MATLAB<sup>®</sup> for the stiffness identification process, and identified values were used to recalculate structural responses using the Newmark- $\beta$  integration method. The simulated structure was subjected to the Cape Mendocino record with peak ground acceleration (PGA) of 0.23 g, with a 10% reduction in pre-yield stiffness applied to the structure at the 10 second mark. Simulated-derived data was recorded at 500Hz.

## 6 RESULTS

Typical responses of the ESDOF of the simulated five-story shear-type concrete structure with a 10% reduction in the linear elastic stiffness at a time of 10 second under the Cape Mendocino earthquake are shown in Figure 3. As shown in Figure 4, in a worst-case sudden failure case,  $\Delta k_0$ , the changes in pre-yield linear elastic stiffness of the structure converge to within 10% of the actual value in less than 2 seconds using 10 taps at a 500 Hz sampling rate. Figure 5 shows that filter approaches faster and smoother to the final values of the pre-yield stiffness changes after damage when higher sampling rates or a greater number of taps are used to identify the stiffness changes.

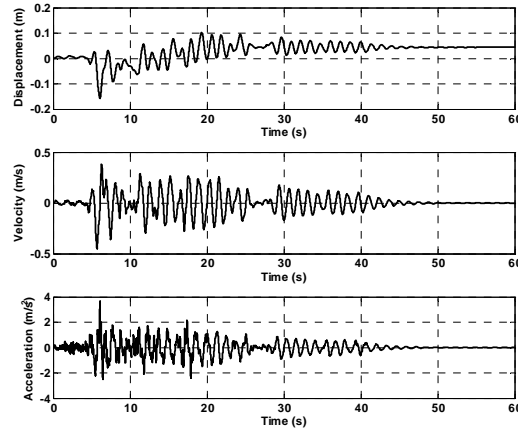


Figure 3. Responses of the simulated structure subject to the Cape Mendocino earthquake and 10% sudden failure

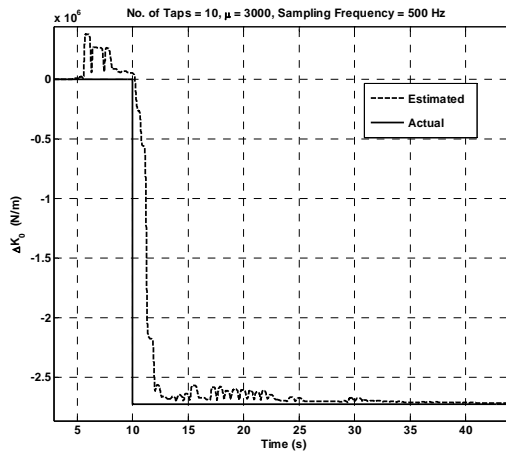


Figure 4. Identified changes in pre-yield stiffness of the simulated structure with 10% sudden failure using adaptive LMS algorithm

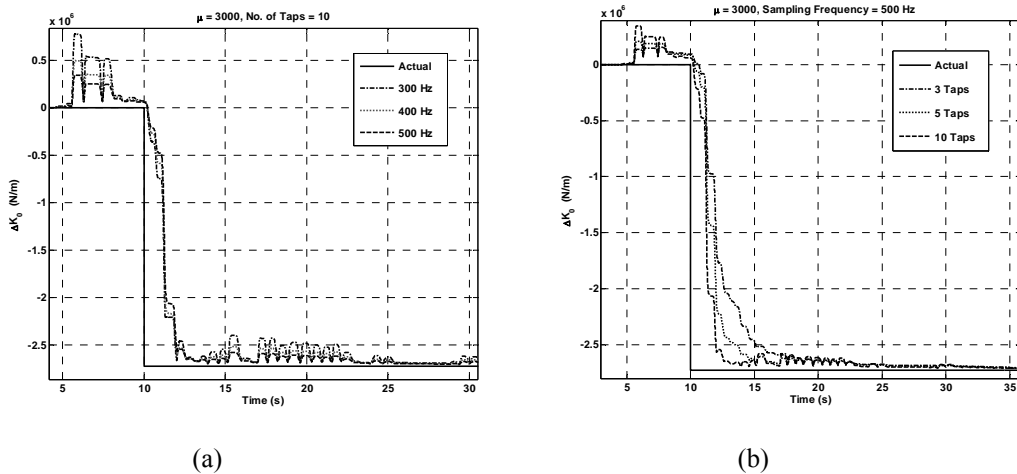


Figure 5. Identified changes in pre-yield stiffness of the simulated structure with 10% sudden failure using adaptive LMS algorithm, (a) at different sampling rates and (b) with different tap numbers

Running the simulation with estimated values for changes in pre-yield stiffness of the structure to obtain identified responses of the damaged structure using the Newmark- $\beta$  integration method and Equations (14) and (15) to get the plastic and permanent deflections of the structure, yields Figure 6.

This figure clearly shows that as the filter approaches its final value for changes in stiffness ( $\Delta k_0$ ), the plastic deflection approaches its actual final value and the error between actual and estimated values for plastic deflections becomes smaller. For the entire record, the ratio between norms of the error signal in estimating the plastic deflections and the displacement signal is less than 2.5%, and the error in identifying the permanent deflection is less than 0.5% of the actual value.

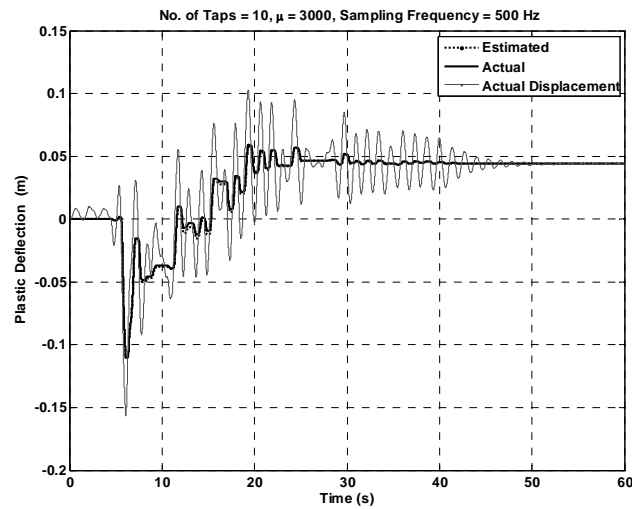


Figure 6. Identified plastic displacement of the simulated structure with 10% sudden failure using estimated changes in pre-yield stiffness of the structure using adaptive LMS algorithm

## 7 CONCLUSION

The developed LMS-based SHM method with a baseline non-linear Bouc-Wen structural model can directly identify plastic deflections and changes in stiffness (modelling or construction error), in real-time. The simulation results show that the algorithm identifies stiffness changes to within 10% of true value in less than 2.0 seconds, and permanent deflection is identified to within 0.5% of actual value.

## REFERENCES

- Baber TT. and Noori MN. 1986. Modelling general hysteresis behaviour and random vibration application. *Journal of Vibration, Acoustics, Stress, and Reliability in Design*, Vol. 108, pp. 411-420, 1986.
- Chase JG, Hwang KL, Barroso LR, and Mander JB. 2004. A simple LMS-based approach to the structural health monitoring benchmark problem. *Journal of Earthquake Engineering and Structural Dynamics* 2004;34(6):575-594.
- Chase JG, Spieth HA, Blome CF, and Mander JB. 2005. LMS-based structural health monitoring of a non-linear rocking structure. *Journal of Earthquake Engineering and Structural Dynamics* 2005;34:909-930.
- Constantinou, MC. and Tadjbakhsh IG. 1985. Hysteretic Dampers in Base Isolation: Random Approach. *Journal of Structural Engineering*, ASCE, Vol. 111, No. 4, pp 705-721, Apr. 1985.
- Hou Z, Noori M, and Amand R. 2000. Wavelet-based approach for structural damage detection. *J Eng Mech* 2000;126(7):677-83.
- Ifeachor, EC. and Jervis, BW. 1993. *Digital Signal Processing: A Practical Approach*, Addison-Wesley 1993.
- Lim, M. and Lim, J. 2008. Visual measurement of pile movements for the foundation work using a high-speed line-scan camera, *Journal of Pattern Recognition Society*, vol. 41, pp. 2025-2033, 2008.
- Loh C-H, Lin C-Y, and Huang C-C. 2000. Time domain identification of frames under earthquake loadings. *J Eng Mech* 2000;126(7):693-703.
- Sato, T. and Qi K. 1998. Adaptive  $H_\infty$  filter: its application to structural identification. *J Eng Mech* 1998;124(11):1233-40.